A multi-criteria approach for spatial modeling of land degradation:

A case study of Babati district in Tanzania

Fred Kizito[1], Kennedy Nganga[1], Lulseged Tamene[2], Job Kihara[1], Nicholas Koech[1],*

[1]International Center for Tropical Agriculture (CIAT) c/o ICIPE Duduville Complex, Off Kasarani Road P O Box 823-00621, Nairobi, Kenya

[2]International Centre for Tropical Agriculture (CIAT), Chitedze Agricultural Research Station, P.O. Box 158, Lilongwe, Malawi

Correspondence: Fred Kizito (e-mail: f.kizito@cgiar.org)

Abstract

The study was conducted in the Babati district of Northern Tanzania where farming and grazing are the main activities and land degradation is a pressing problem characterized by high erosion prevalence and soil degradation risk. Modeling to identify areas prone to land degradation was carried out with the integration of Remote Sensing and GIS operations, specifically overlay analysis by combining several causative factors in an ARC/INFO environment. The first emphasis was the identification of areas with physical degradation which corresponded with the highest erosion hazard, categorized based on remotely sensed and field survey data. This effort resulted in the roll out of an add-on tool box in ArcGIS for erosion hazard assessment (accessible at: ciat.cgiar.org). Field survey data was obtained through routine field verification and validation visits to ground truth results from the erosion hazard assessment. The resulting physical degradation (vegetation degradation and soil erosion hazard) analyses were then compared and overlaid over the chemical degradation analyses (soil organic carbon, salinization and cation exchange capacity) to attain a land degradation product.

The study results revealed seasonal differences in the erosion hazard index and also resulted in four degradation categories: Not degraded, Transitional zone non-degraded, Degraded and Severely Degraded. Based on analyses conducted to identify the predominant pixels of a given degradation category for each of the land uses in Babati; results revealed that cultivated land was predominantly degraded (37%) while forests (15%) and grasslands (47%) were in the transition zone non-degraded category. Cultivated lands form the mainstay of the populations in the study area yet these areas showed high levels of land degradation resulting from high soil losses and deficiency of nutrients and soil organic carbon in the soils. Given that the transition zone non-degraded accounted for about 60% of the area being on the borderline to potential degradation. Results revealed the need to carefully design degradation recovery plans to prevent losing these valuable yet vulnerable lands. It is hoped that land degradation assessment results emerging from this study will provide relevant guidance for decision makers to take the necessary actions to target restoration options for both the most vulnerable yet economically beneficial degraded areas.

1. Introduction:

Land degradation can be described as the reduction in the present and prospective land quality and production, due to natural or anthropogenic dynamics (Rabia, 2012; Alexakis et al., 2012). Earlier work on land degradation surmised that it leads to long-term decline in soil's quality, productivity and beneficial functions of value to humans (Doran and Parkin, 1994; Lal, 2001). Soil erosion by water is one of the most significant forms of land degradation that affects sustained productivity of land use yet, its extent, severity, economic and environmental impacts remain obscure. Moreover, the global and regional land area affected by land degradation are tentative and subjective (Mallick et al., 2014). Currently, there are two

approaches commonly in use in the estimation of soil loss for land degradation assessment. First is the assessment of soil erosion on the basis of a point or a single plot (Kovar et al., 2011; Othman & Ismail, 2012; Peter et al., 2014), and the second approach takes into account the geographical patterns of the area of interest (Parveen & Kumar 2012; Mallick et al., 2014). The limitation of first approach is the difficulty of understanding the erosion phenomena in terms of spatial patterns and relationships between units of the land under study, especially at a landscape level. Accordingly, for effective restoration planning, the latter methodology would be preferred, where both remote sensing and GIS techniques aid in the analytical processes (Alexakis et al., 2012; Csafordi et al., 2012). This study employed the second approach to assess physical land degradation by estimating soil loss areas and vegetation degradation in the landscape and integrated this with chemical soil degradation associated with soil organic carbon, cation exchange capacity and soil salinization. The goal of this study was to design a geo-processing model capable of simulating various input datasets and outputting a guidance map for land degradation in the study area. The specific objectives of the study were three-fold: (i) Create an ArcGIS add-on geo-processing (GP) tool for erosion hazard modelling; (ii) Produce maps showing erosion hazard potential of different areas across different seasons of the year in Babati District; (iii) Develop a land degradation guidance map that identifies hotspots of physical and chemical degradation for targeting economically beneficial restoration activities.

2. Materials and Methods

2.1. Site characteristics:

Figure 1: Location of target sites in the villages of Long, Seloto and Sabillo in Babati District, Tanzania

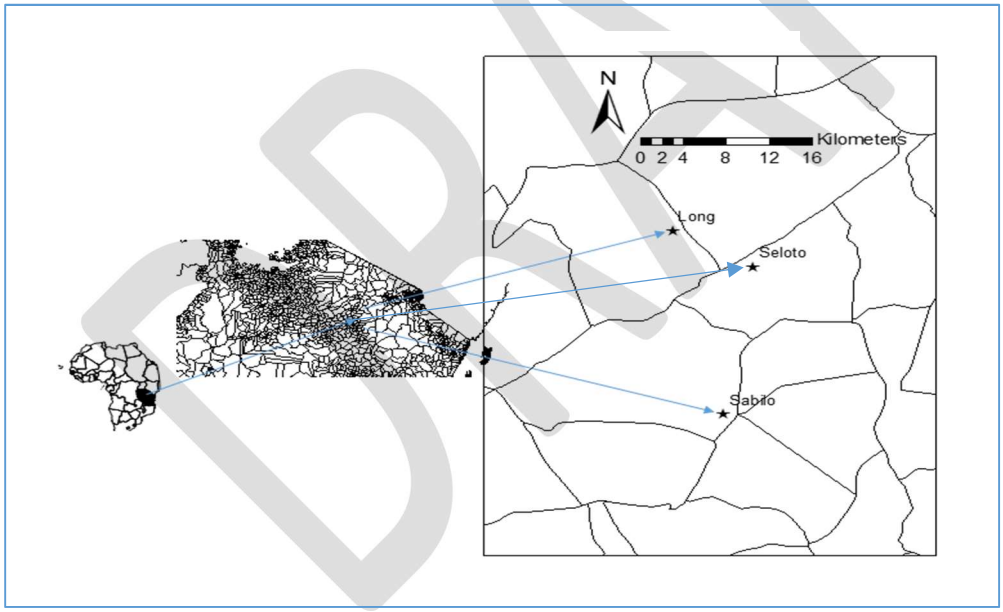

The study was conducted in the Babati district of Northern Tanzania (Fig. 1), located between the latitudes 3° and 4° south and the longitudes 35° and 36° with an altitude between 1,650 to 2,250 meters above sea level. The Region is a part of the Great Rift Valley and the landscape is characterized by mountains, undulating hills and plains. The precipitation varies with the altitude and ranges from 1200 mm/year in the highlands down to 500 mm/year in the lowlands. The rains are bimodal with the short rains beginning in November and ending in the December/January period while the long rains begin in February and end in May. The short and the long rains are often connected and undistinguishable (Bishop-Sambrook, 2004). The main food crops are maize, paddy, sorghum and common beans while coffee, pigeon peas, sunflower and sugarcane are the most important cash crops (Ringo et al., 2002). The predominant cropping pattern

for the long rains is maize inter-cropped with pigeon peas or beans. Most farmers are not able to cultivate crops during the short rains as they used to, due to a changed and more unreliable short rain period (Bishop-Sambrook, 2004). The soils are mainly of volcanic origin and range from sandy loams to clay alluvial soils. The content of organic material and availability of phosphorus is generally low across the district (Jonsson, 1996). Many farmers in Babati District are agro-pastoralists and the number of livestock in the area is high, livestock rearing constitutes about 35% of the overall land use in the district (Ringo et al., 2002).

2.2. Erosion modeling

Erosion hazard modeling needs to consider a variety of factors that influence the likelihood of erosion occurring in an area which requires that both the erodibility of the soil, as well as the erosivity caused by weather be taken into consideration (Prasannakumar et al., 2012). However, it is becoming increasingly clear that the anthropogenic influence caused by man's activities are critical in determining soil erosion hazard (García-Ruiz, 2010). As such socio-economic factors need to be considered when looking at the broader issues that propel land degradation. In this study some of the factors considered by the Modified Universal Soil Loss Equation (MUSLE) were used as the base of the biophysical factors to be included in our model (Agele et al., 2013; Kumar & Kushwaha, 2013). To the commonly considered biophysical factors were added socio-economic considerations that play a role in promoting soil erosion.

Against this background, we developed an erosion hazard index (EHI) approach to evaluate the erosion sensitivity of landscapes and map erosion hotspots. The EHI model is a soil erosion risk model that defines the relative hazard of each grid (unit area) in a given study area is exposed due to the causative factors of soil erosion. The EHI is a step further to some of the above 'index-based' semi-qualitative approaches as it is designed to map the spatial variability of soil loss. Though the model is based on quantified biophysical data such as rainfall amount, soil type, topography and vegetation indices, the model is semi-qualitative in nature in that it defines the risk according to a scale of severity rather than using quantitative figures. Various other studies such as PSIAC (1968); Hadley et al. (1985); Verstraeten et al. (2003); Lawrence et al. (2004); de Vente et al. (2006); Wu and Wang (2007), Tamene et al. (2006a, 2011), applied a similar technique in their assessment of soil erosion risk and map hotspot areas of erosion that require prior intervention Based on a number of thematic GIS layers and remote sensing data, they integrated a variety of physical and managerial factors that are dominant in water-based soil erosion in their study areas.

The EHI model borrowed heavily from the USLE in terms of biophysical factors. However, in the EHI we have included other socio-economic drivers that play significant role in initiating and/or aggravating soil erosion and land degradation (Bhushan and Rai, 2004). For instance, physical infrastructure such as dirt roads have shown to have a huge effect on soil erosion (Forman, 1998). Harden (1992) showed that roads and footpaths were among the most active run-off generating components in hilly landscapes and thus deserve to be incorporated into erosion risk models especially at the watershed scale. Due to this, models such as spatially distributed soil erosion and sediment delivery model (WaTEM/SEDEM have been designed to capture the impacts of footpaths and field boundaries on sediment yield (e.g., (e.g. Van Oost et al., 2000; Van Rompaey et al., 2001, 2005, 2007; Verstraeten et al., 2002, 2007; Verstraeten and Prosser, 2008). Other findings also showed that road embankments contribute heavily to soil erosion and need to be included in soil loss assessments (Cerda, 2007). The distance from roads has also been shown to be a determinant in soil erosion as indicated by several studies (Shi et.al, 2008, Mohammadkhan, 2011).Similarly water channels such as streams and rivers have been found to contribute to erosion (Hooke, 1979). For instance, Wolman (1967) showed that cycles of erosion and deposition usually occur within such channels, a finding that was dovetailed by Trimble, 1997. Similar to distance from roads, distance to rivers is also crucial in assessing the sensitivity to erosion of landscapes (de Vente et.al, 2008; Tamene et al., 2006). The

effect of land use and land cover changes as well as plant cover/biomass on soil erosion has also been extensively studied (Zuazo et.al, 2008; Nunes, 2011; Bakker, 2008; Bork, 2003).

Population pressure as a factor of land degradation has been widely studied and shown to be a critical factor in the occurrence of degradation processes. One of these studies carried out in Eastern Africa by Grepperud (1996) tested the population pressure hypothesis, which states that under comparable physical conditions heavily eroded areas tend to occur in highly populated regions. The findings showed that as both human and livestock population pressures exceed a certain threshold there is rapid degradation of land. Pascual & Barbier (2003), also investigated the population pressure hypothesis and found that particularly for poorer households and communities, population density increase led to an increase in clearing of forest land and was an important driver for soil degradation.

The overlay analysis was conducted in two parts, with sub-models of the major factors being created prior to their linking up to form the larger overall model. This was done to independently include the effect of each of the different factors that contribute to erosion. For instance soil texture as a factor is independent of a factor such as topography. Each of these factors contributes an independent component to the erosion hazard which is why they are separately modelled before eventual summation into a more global model. This is a commonly used technique in solving multi-criteria problems through weighted overlay operations (Carver, 1991). The erosion model used by this study can be mathematically expressed by the following additive equation:

$$EHI = PD(w1) + LC(w2) + SC(w3) + T(w4) + P(w5) + CF(w6)$$

Where:

EHI is the erosion hazard index, a scale showing the relative risk of erosion across the landscape in order of increasing magnitude.

PD is the population density component. Composed of both human population density and livestock population density.

LC is the land cover component. It is composed of both the land use as well as biomass.

SC is the soil characteristics component. Determined by the soil texture property.

T is the topography component. It includes both the slope and the stream power index which is an extended proxy of slope length.

P is the precipitation component. It considers the effect of rainfall erosivity on erosion risk.

CF is the channel features component. It is composed of geographic features such as roads and rivers which are vulnerable to erosion when they act as water conduits.

w1 – w6 are the associated weights that each factor is multiplied by before addition.

The schematic in Figure 2 describes the methodology applied in the execution of these analyses and further shows the linkage of the erosion hazard index to chemical soil degradation.

2.3. Input layers

The layers used in this study were selected to best model different factors represented by the sub-models as exemplified in Table 1. Table 1 provides a breakdown of the datasets used in the component sub-models where each was assembled separately using the input layers that were relevant to the erosion factor being modelled. In order for some sub-models to be built, it was necessary to derive extra datasets from some of the original layers. An important consideration was that the various layers represented different information and were in different measurement units. In order for these different layers to be combined within sub-models, the layers had to be standardized to a common scale and unit of measurement. Therefore harmonization of data sets using raster reclassification tools was conducted on the input layers. This methodology has been used for soil erosion risk studies (Rabia, 2012; Jiang, 2013).

Further details on model design and details of the datasets has been provided as supplemental material in Annex 1.

Table 1: Layers included in the model and their sources.

Layers	Dataset
Biomass	NDVI raster from SPOT VGT
Soil Texture	Soil texture raster from ISRIC soil database
Slope	Derived from SRTM 30m DEM
Stream Power Index	Derived from SRTM 30m DEM
Precipitation	Rainfall dataset from TRMM
Population Density	Population dataset from NASA GPW
Livestock Density	Livestock density dataset from FAO STAT
Land Use / Cover	Land cover land use dataset from GLC 30
Roads	Road layer from Digital Chart of the World
Rivers	Hydrology layer from Digital Chart of the World
Distance to Roads	Generated from the roads layer
Distance to Rivers	Generated from the rivers layer

2.4. Weighting procedures and criteria

In both the sub-models as well as the overall model, the input layers contribute differently to the factor being modeled. As such, it was necessary that the input layers be assigned weights corresponding to their influence before they were analyzed jointly with others. In this study, weights were allocated according to the analytical hierarchical process (Banai, 1993; Schmoldt, 2013, Yalcin (2008), Komac (2006), and Nekhay et.al (2009). The analytical hierarchy process (AHP) is a means of mathematically assigning weights to the

different factors in a multi-criteria decision analysis (Forman and Gass, 2001). Pairwise comparisons are used to rate the different factors and assign weights based on the outcome of the ranking (Winkler, 1990).

Field observations were done in July 2015 to collect training data for the AHP process in the study area. Points to be visited for training data were selected using a stratified sampling strategy. Each of the major contributing factors outlined in Table 1 was quantified at each of these sampled locations. The observed data at all the visited points was used to facilitate the pairwise comparisons in the analytical hierarchical process and thus derive the relevant weights for the input factors. The susceptibility of a point to erosion was based on the strength of the contributing factors at the point as well as the observed health of the surrounding land. This approach takes into consideration the contextual setting of a location. For instance a point in a neighborhood with rills or a gulley would be determined more likely to get eroded compared to a similar point surrounded by pristine lands. From this stratified sampling, 40 locations with varying levels of erosion hazard were obtained to provide data for the pairwise ranking. The resulting rank was then used to weigh the major factors in the model according to the importance of each relative to the others.

The analysis in this study was disaggregated based on a seasonal criterion in order to take into account the phenological changes that occur between seasons while teasing out the contribution of rainfall to degradation trends within these landscapes. Model runs were conducted at two distinct periods, using data from the peak of the dry season (Table 2) and the same model run conducted using data from the wet season (Table 3). The datasets that contained seasonal variations useful in distinguishing the wet from dry season were precipitation and biomass. Since a major part of this analysis utilized remote sensing data, the phenological differences between the seasons were accurately captured within our data set. This disaggregated approach allowed us to accentuate these differences allowing for closer examination and comparison of erosion hazard between seasons.

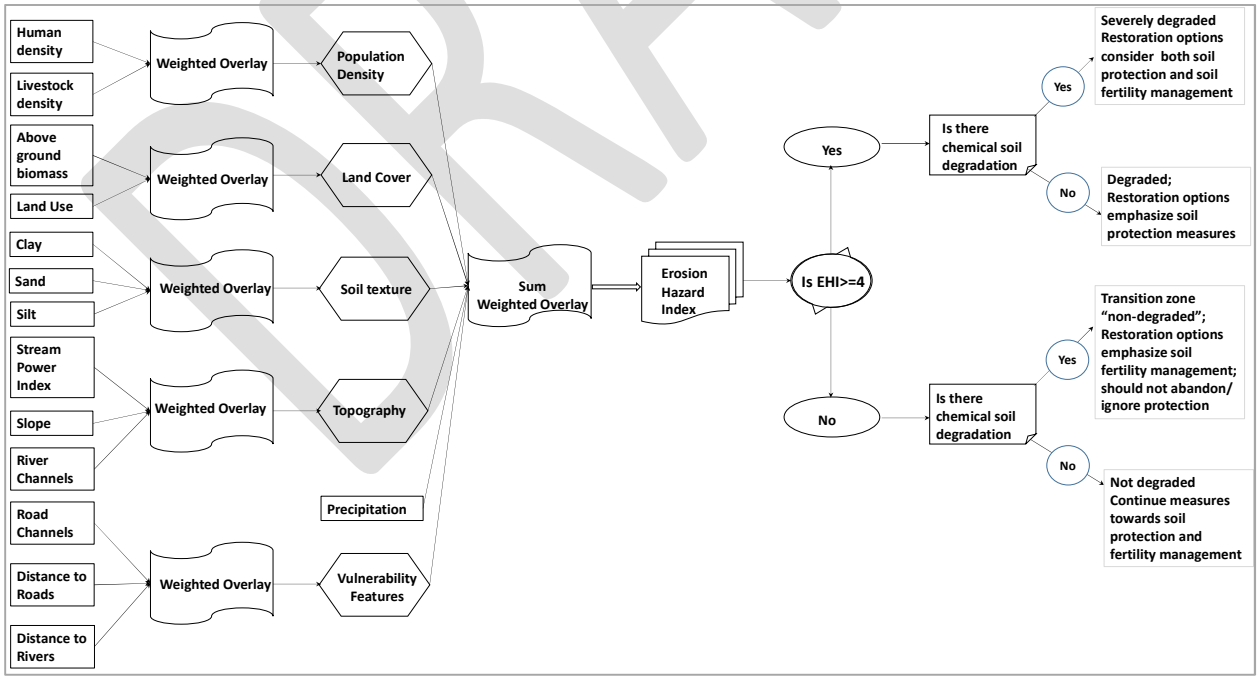

Figure 2: Schematic logic work flow for erosion hazard modeling with linkage to overall land degradation assessment and management options.

Mendas and Delali, 2012 used weighted sum methods for land suitability support mapping of agricultural areas in Algeria. In our study, the outputs of the sub-models were similarly combined with an additive weighted overlay analysis, a type of spatial analysis that is commonly used to solve multi-criteria problems such as that being addressed by this study. The outputs from the sub-models, which form the input datasets in the overall analysis, are multiplied by the relevant weight identified for each factor. The resultant raster data from this process are then combined to produce the final output raster which represents erosion hazard for each cell. In this raster, the higher the cell value the higher the erosion hazard. Features such as water bodies were masked in the input layers to exclude them from the analysis.

The weights assigned to factors in the model are not universal since they vary between geographical locales. In lieu of pre-existing data from the literature, this necessitates that a field mission be undertaken to observe the study area and assign weights to the model thereafter. One of the advantages of this flexibility is that the model can be customized to fit any area since its core parameters can be localized.

Table 2: Weights assigned to factors in the dry season model based on field observation data and AHP.

Contributing factor	Percent weight
Vulnerable features	5
Topography	30
Land cover	10
Population density	45
Soil characteristics	5
Rainfall	5

*Vulnerable features are pre-existing water channels such as seasonal rivers, dirt roads, and trenches/gulleys where water runs off during rain storms. These features tend to have exposed walls on the sides of the channels with little vegetative cover, which makes them highly vulnerable to further erosion. The fact that they also act as the natural pathways for water means they are more likely to be exposed to the main agent of erosion compared to other areas.

Table 3: Weights assigned to factors in the wet season model based on field observation data and AHP.

Contributing factor	Percent weight
Vulnerable features	30
Topography	25
Land cover and use	25
Population density	5
Soil characteristics	5
Rainfall	10

2.5. Land Degradation assessments

2.5.1. Soil Organic Matter

Soil organic carbon (SOC) is a potential soil fertility indicator for regulating soil functionality in tropical farming systems, if certain SOC fraction thresholds are below or above critical levels, the desirable soil functions may be reduced or improved respectively. Krull, Skjemstad and Baldock (2004) discussed some of the minimum and maximum thresholds of SOC, above or below which the effects of SOC on soil functions are noticeable. However, Sparling and Schipper (2002) argued that other than defining such maximum values, it is reasonable if minimum SOC levels are established to inform the farming community on levels below which there would be loss of important soil characteristics. In this study; we used the latter approach and specified the minimum threshold as being about 20.5 g kg-1 (~2%) SOC level as appropriate for supporting crop production in SSA (Berger, 1987; Musinguzi, 2013).

2.5.2. Cation Exchange Capacity

Cation-exchange capacity (CEC) is the maximum quantity of total cations that a soil is capable of holding, at a given pH value, available for exchange with the soil solution (with most of the soil's CEC occurring on clay and humus colloids). The CEC is used as a measure of fertility and nutrient retention capacity and is expressed as centi-mol of Hydrogen per kg (cmolc/kg or 100 meqc/100g). These attributes serve as surrogate indicators for the exchangeable bases (Ca, Mg, Na and K) in the soil matrix (Shakesby et al., 2002). The higher the CEC the more clay or organic matter present in the soil. This usually means that high CEC (clay) soils have a greater water holding capacity than low CEC (sandy) soils. Low CEC soils are more likely to develop potassium and magnesium (and other cation) deficiencies. Similar to work conducted elsewhere on CEC thresholds, this study set a minimum value of 10 cmolc/kg (van Noordwijk, 1997 and Murage, 2000).

2.5.3. Analysis of EHI and soil chemical properties

The study used a hierarchical approach by building on results from the erosion hazard index (EHI) as a base layer for land degradation assessments. It hinged on the fact that soil erosion is one of the most significant forms of land degradation that affects sustained productivity of land use (Alexakis et al., 2012; Mallick et al., 2014). However, the assessment of physical soil losses only forms part of the story because quite often, there is little significance accorded to the role of the nature and properties of soils within agricultural landscapes in maintaining ecosystem integrity. Therefore, in addition to the EHI, this study further assessed soil chemical properties specifically the Soil Organic Carbon (SOC) and the Cation Exchange Capacity (CEC). The soil chemical data was obtained from sentinel sites combined with collated and harmonized soil legacy data provided by ISRIC (ISRIC, 2014). As exemplified by the conceptual matrix (Figure 2); the EHI was categorized into 7 distinct categories (1-2: no erosion; 3: low; 4: moderate; 5: high; 6: excessive; 7: severe. For the degradation assessments, we used values >= 4 as a threshold to signal concern for soil losses; any pixels that showed < 4 did not pose a threat to erosion.

The thresholds for SOC (2%) and CEC (10 cmolc/kg) outlined in Sections 2.5.1 and 2.5.2 were used to analyze the % of pixels from the EHI layer with raster algebra that were meeting criteria outlined in Table 4. It should be noted that there are borderline cases that could result in missing data if such calculations are conducted on Raster images which was compensated for by ensuring that all values of pixels represented in the EHI were included through computations that involved converting the borderline pixels.

Table 4. Procedural analysis of EHI, SOC and CEC for land degradation categories

EHI level (Pixels)	SOC (%)	CEC (cmolc/kg)	Raster Algebra	Category generic description
< 4 Below moderate	>=2	>= 10	("EHI"<4)&("CEC.tif">= 10)&("SOC.tif" >=2%)	*Not Degraded* (low erosion risk and good fertility status)
>= 4 Above moderate	>=2	>= 10	("EHI">=4)&("CEC.tif">= 10)&("SOC.tif" >= 2%)	*Transitional zone* (high erosion risk but good fertility status)
< 4 Below moderate	<=2	<= 10	("EHI"<4)&("CEC.tif"<= 10)&("SOC.tif"<=2%)	*Degraded* (low erosion risk but poor fertility status)
>= 4 Above moderate	<=2	<= 10	("EHI">=4)&("CEC.tif"<= 10)&("SOC.tif" <=2%)	*Severely degraded* (high erosion risk and poor fertility status)

2.6. EHI Data analysis

Validation data was collected in the field to cross-check the accuracy of the model output. This was done during the period of mid to late 2015, specifically around the months of July to September. A random sampling strategy was used to generate 40 random points for field visit to validate the model. The points were generated using the *genrandompnts* command of the Geospatial Modelling Environment tool and navigated to using handheld GPS units. Sample points were visited and the prevailing land cover, amount of biomass, slope intensity and degradation conditions noted. The neighborhood around a sample point was also observed in each of the cardinal directions similar to what was done when collecting the training data. From these indicators, coupled with a general visual analysis of the site, the erosion hazard was determined and classified using simple categories.

The model output was compared against the field data and statistical indices using the Cohen's kappa coefficient were computed. This statistic allows for measuring inter-rater agreement on categorical items while accounting for agreement due to chance alone.

Given 2 raters where each classifies X items into N mutually exclusive classes, the equation for kappa is stated as follows:

$$k = \frac{Po-}{1-Pe} = 1 - \frac{1-Po}{1-Pe} \qquad \text{Equation 1:}$$

Where Po is the relative agreement among raters, and Pe is the probability of chance agreement. $\kappa = 1$ when the raters are in full agreement while $\kappa \leq 0$ when there is zero agreement among the raters other than what would be expected by chance (as given by Pe) (Cohen, 1960).

Additionally, the model output were examined against the contributing factors to better understanding the dynamics between erosion and its causative agents. A covariance matrix is used to measure how changes in one variable are associated with changes in another. It helps define the degree to which 2 variables are linearly associated. In the context of this study, a covariance matrix between the erosion hazard and the contributing factors was computed. To assess the strength of associations, a correlation matrix was computed to scale the covariance matrix to between 0 and 1 in order to represent no linear association and perfect linear association respectively. Only tabulated values for the correlation matrix are provided in Table 5.

2.7 Seasonal variations

Further analysis aimed to understand how erosion hazard changed between the wet and dry seasons. Given that the erosion hazard model has N classes of erosion hazard, it was critical to find out if there were transitions between these erosion classes across the seasons. For this analysis, fractal dimensions were used to show how the erosion hazard changes across the landscape from one class to another as the seasons change.

Fractal dimension is a measure of shape complexity derived by examining its perimeter against its area. It is defined as the ratio of the log of the number of new parts N, to the log of scale, ε. The mathematical equation for calculating fractal dimension DF is:

$$D_F = \log N / \log \varepsilon \qquad \text{Equation 2:}$$

In this study, the fractal dimension index was used to give an indication of how fragmented the erosion hazard classes were at the peak of each season. By subtracting the fractal dimension of the dry season from that of the wet season, we can determine how the degree of fragmentation of the erosion hazard classes changed from the wet season to the dry season. This acts as an indicator of transitions between erosion hazard classes from the wet season to the dry season. The following formula was used to identify class transitions, C_T, and gives an indicator of the magnitude of change.

$$CT = DFwet - DFdry \qquad \text{Equation 3:}$$

A positive result establishes that the fractal dimension has reduced across the seasons. This indicates less fragmentation of the erosion hazard classes in the dry season compared to the wet season. What this indicates is that during the dry season erosion hazard concentrates into a few classes that dominate the landscape. However, in the wet season the dominance of these classes is diminished as erosion hazard across the landscape distributes into other classes. A negative result from the formula would indicate that it is the dry season that experiences more class fragmentation. Thus we are able to capture transitions between erosion hazard classes across the seasons. The numerical value of CT indicates the magnitude of the class transitions across seasons. Fractal dimension index metrics were computed at the class and landscape level for both erosion hazard maps.

3. Results and discussions

3.1. The Dry Season Model

Results from this model show that places with high livestock populations are at the highest risk of erosion during the height of the dry season. This result is in line with the validation data from the field visit which identified livestock-related degradation as being the strongest erosion determining factor during dry seasons. While other factors such as topography and land use are significant, it is areas that had higher livestock density that face bigger risk to soil erosion during the dry season. Figure 3 shows a map of the dry season erosion hazard for Babati district of Tanzania. From the correlation matrices, the association between the different causative factors and the erosion hazard was shown as depicted in Table 5.

Table 5: Key to deciphering variables in correlation matrix*

Value	Variable	Dry Season Correlation matrix of erosion hazard index and causative factors	Wet Season Correlation matrix of erosion hazard index and causative factors
1	Erosion Hazard Index	1.00000	1.00000
2	Land Use Land Cover	0.13724	0.28441
3	Biomass	0.27540	0.65576
4	Livestock Population Density	0.80084	0.20845
5	Human Population Density	0.27539	-0.00992
6	Stream Power Index	-0.89780	-1.20689
7	Slope	0.30089	-0.06253
8	Road Channels	0.07595	0.22859
9	River Channels	0.04201	0.34259
10	Distance to Roads	0.18148	0.13219
11	Distance to Rivers	0.06730	0.18937
12	Silt	-0.10642	0.12178
13	Sand	-0.00574	0.07481
14	Clay	0.06906	0.02166
15	Precipitation	0.18495	0.15817

* A kappa coefficient of 0.83 was obtained from field validation using ground truthing data. This indicates a confidence of 83 percent in the model's ability to predict erosion hazard hotspots on the ground.

3.2. The Wet Model

Results from this model show that vulnerable features which act as water-conducting channels such as seasonal rivers and roads are at the highest risk of erosion during the wet season. However they occupy a small percentage of the total land area which makes their impact less adverse than other land uses such as agricultural lands. Areas with steep slopes are also indicated to be highly vulnerable, as well as areas with sparse vegetation cover. This is particularly critical in croplands where the slope is rather steep. However, it is the channels where water runs that are at the highest risk of being eroded during the wet season, such as gulleys, dirt roads, seasonal streams. These results are consistent with the validation data from the field visit which identified these areas as displaying high susceptibility to erosion. Figure 4 shows a map of the wet season erosion hazard for the same district as above. The results of the analysis per season are shown in Table 6.

Table 6. Seasonal fractal dimension index

EHI Class Metrics	Mean	Area-Weighted Mean	Median	Range	Standard Deviation	Coefficient of variation	Perimeter area fractal dimension
Dry season							
2	1.0246	1.0285	1.0092	0.2319	0.0361	3.5274	1.4477
3	1.021	1.2244	1	0.2476	0.0380	3.7263	1.5427
4	1.0217	1.2617	1	0.2956	0.0382	3.7387	1.5634
5	1.0237	1.2127	1	0.2690	0.0399	3.8960	1.5822
6	1.0232	1.1395	1	0.1909	0.0398	3.8926	1.6000
7	1.0354	1.1047	1	0.1394	0.0535	5.1689	1.7171
Landscape	1.0227	1.2302	1	0.2956	0.0389	3.8074	1.5592
Wet season							

2	1.0212	1.1175	1	0.2108	0.0363	3.5546	1.5616
3	1.0273	1.2043	1.0092	0.2651	0.0415	4.0358	1.5234
4	1.0282	1.2510	1.0092	0.2846	0.0448	4.3593	1.5613
5	1.0306	1.1882	1.0092	0.2708	0.0463	4.4931	1.6131
6	1.0246	1.0875	1.0092	0.2047	0.0364	3.5526	1.5976
7	1.0041	1.0057	1	0.0092	0.0046	0.4563	NA
Landscape	1.0277	1.223	1.0092	0.2846	0.0430	4.1836	1.5675

CT = DFwet - DFdry = 1.5675 – 1.5592 = + 0.0083

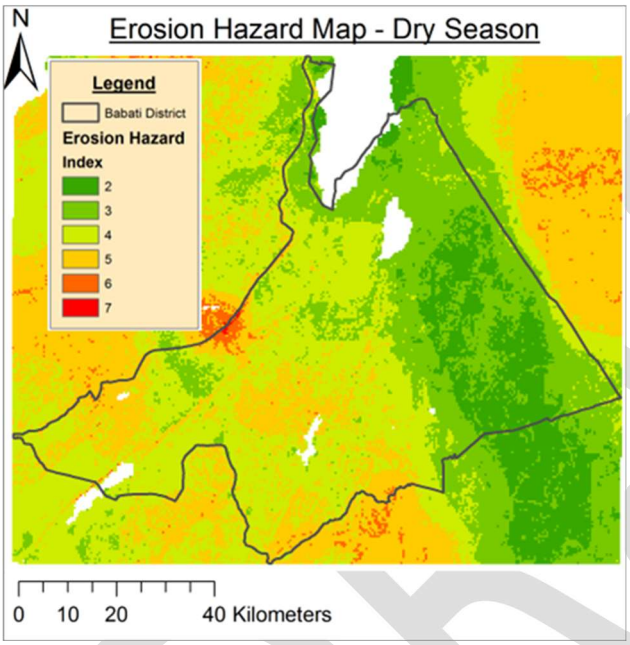

Figure 2: Dry season erosion hazard map.

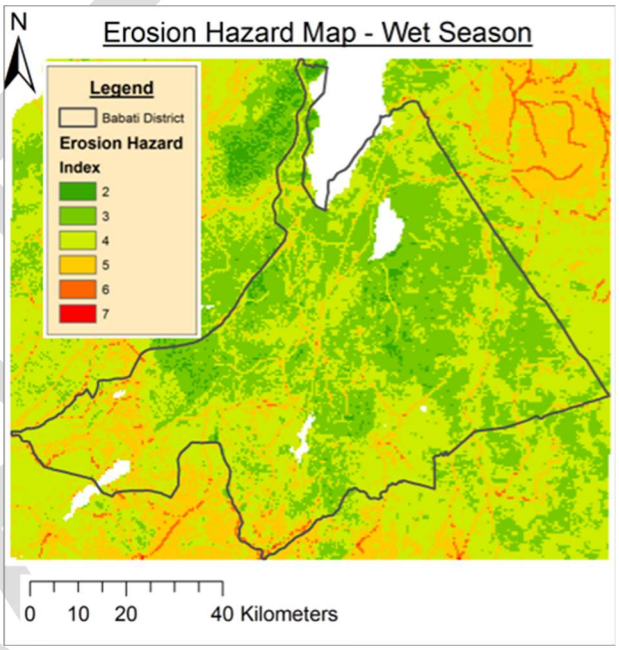

Figure 3: Wet season erosion hazard map.

3.3. Land Degradation assessments

As portrayed in Table 4, using the functions outlined for raster combinations of EHI and soil chemical properties (Figures 4, 5 and 6), the results revealed four distinct degradation categories namely i) Not Degraded; ii) Transition Zone Non-degraded; iii) Degraded; iv) Severely Degraded and resulted in the land degradation map shown in Figure 7. The categories are further explained in the conceptual framework (Figure 2). The target sites shown in Figure 7 indicate that they were interspersed among the different degradation categories. We present a bird eye's view of Babati District and the positioning of the target sites in the landscape in relation to their degradation classes along a topographic gradient in Figure 8 to visually complement the degradation map in Figure 7.

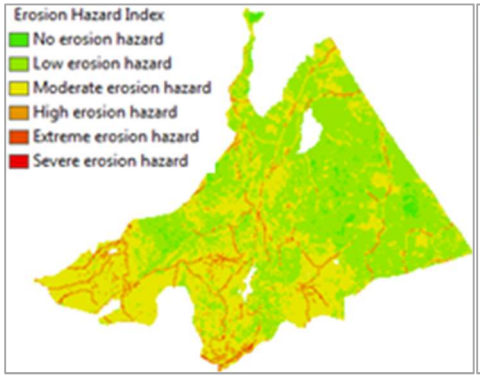

Figure. 4: EHI base layer (Wet season)

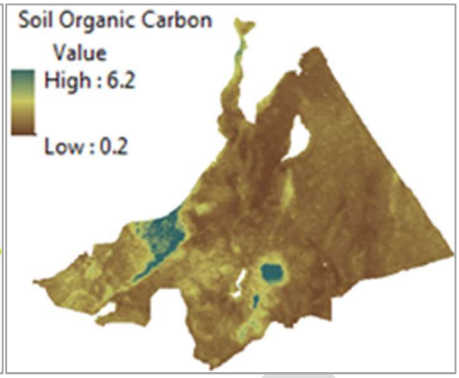

Figure. 5: Soil Organic Carbon

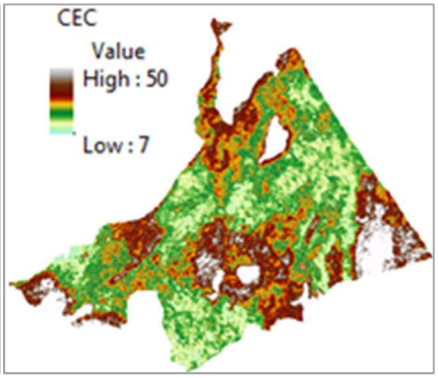

Figure.6: Cation Exchange Capacity

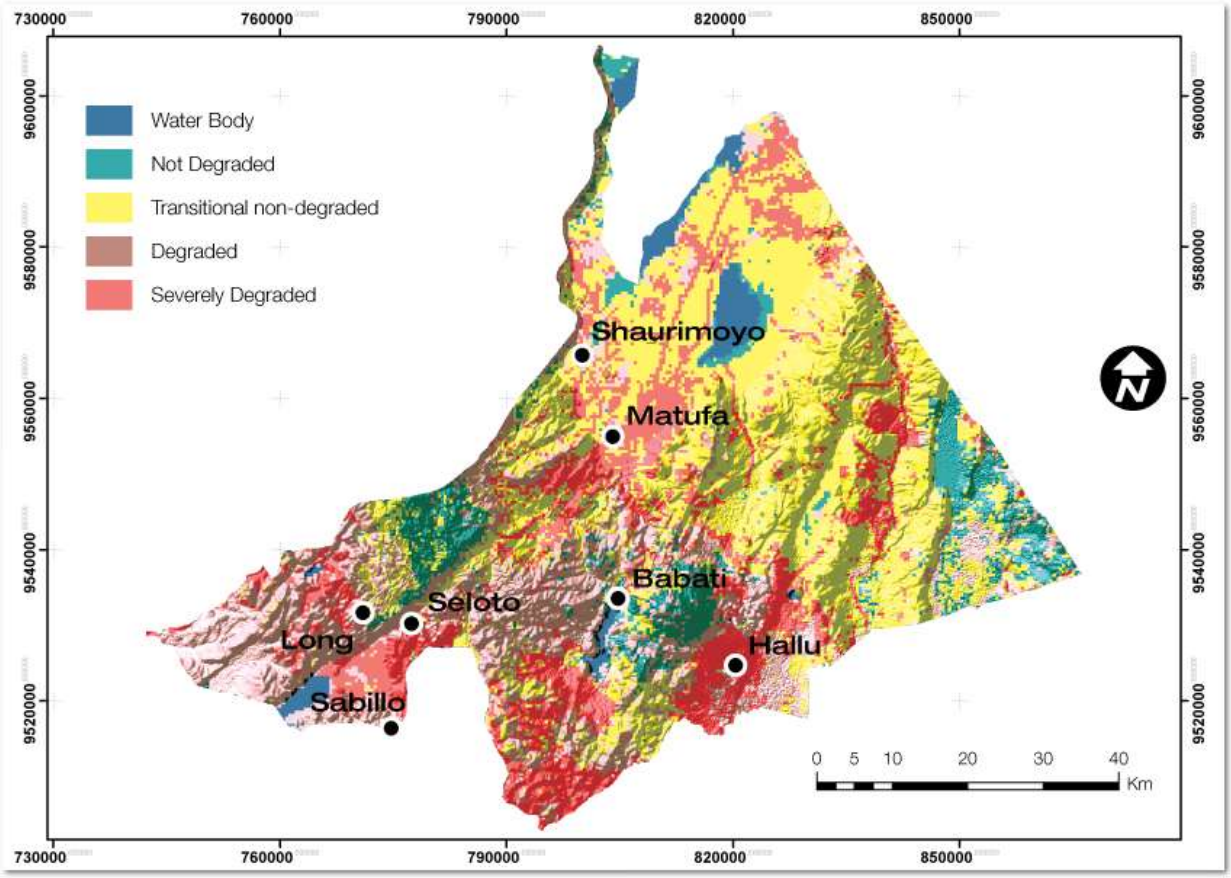

Figure.7: Land degradation map for Babati District, Tanzania

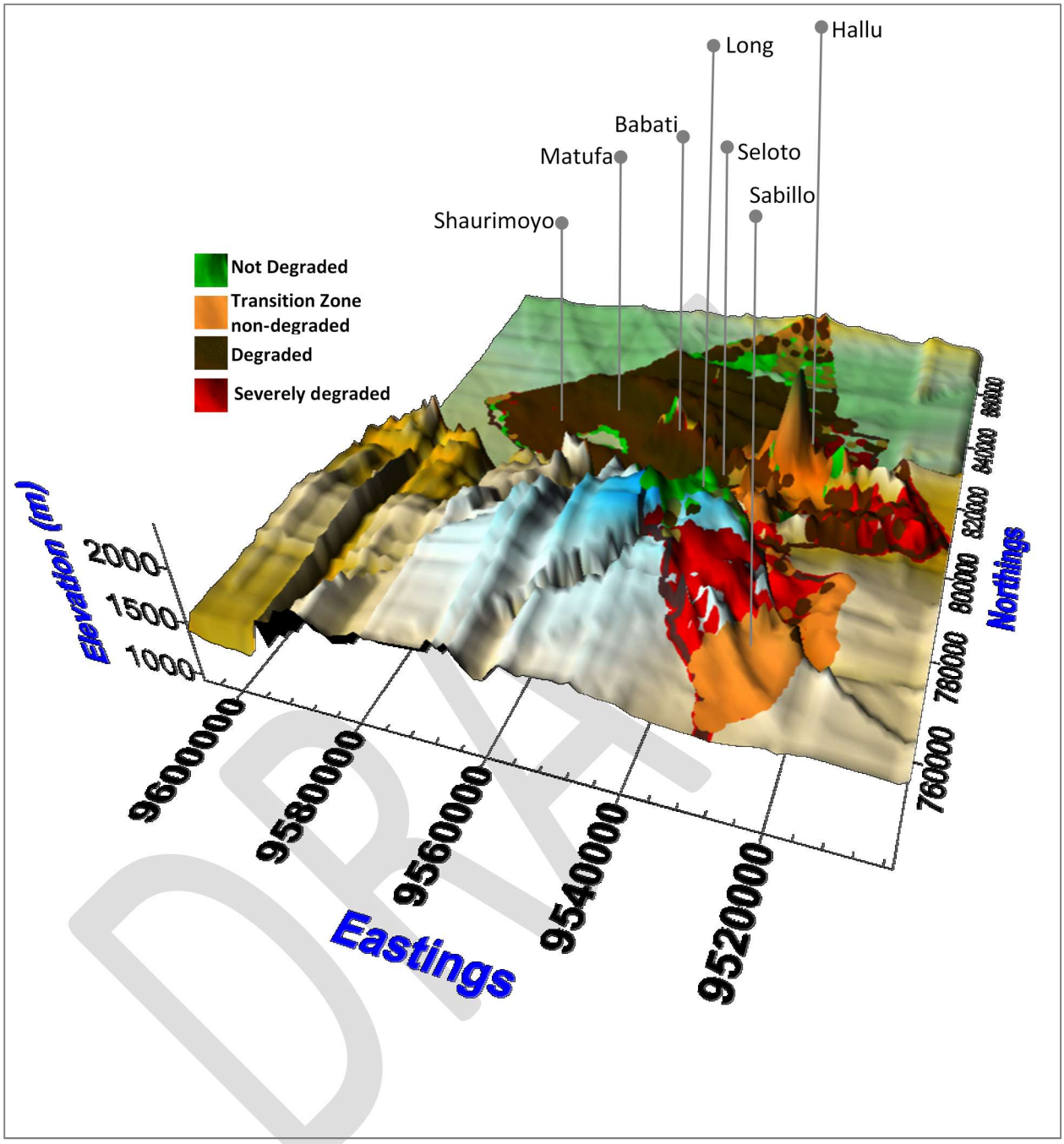

Figure.8: Bird eye's view of degradation in target sites within Babati District, Tanzania

In relation to Figures 7 and 8; the four degradation categories occupied the following proportions of the landscape: 9% (Not degraded); 42% (Transition Zone Non-degraded); 26% (Degraded) and 23% (Severely Degraded). Beyond the proportions revealed by these percentages for each category, the relative distribution of land degradation based on the land use type is provided in Figure 9. Figure 9 presents the dominant degradation category observed for each land use type.

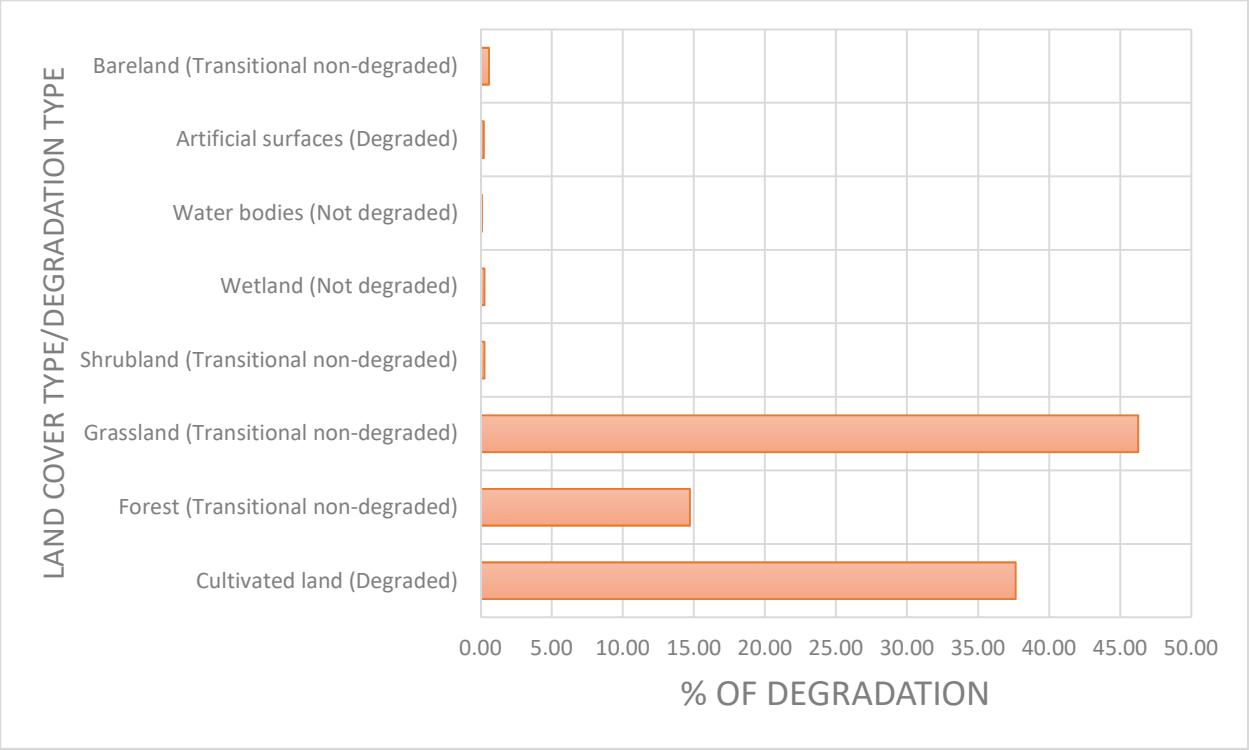

Figure.9: Predominant degradation category for the different land use types in Babati, Tanzania

Results from Figure 9 depict the category of degradation based on the predominant percentage of degraded area for a given land use type. Evidently grassland (47%) and forest (15%) are two land uses that show high percentages of the transition non-degraded category while about 37% of the cultivated lands fall under the degraded category.

Figure 10 further represents the land degradation categories by teasing out the relationship between the population density (human and livestock) and the degradation classes among five selected target sites. For Babati, there was higher human population density within the not degraded and transition zone non-degraded areas while livestock population density outnumbered the human population with a fair distribution across the 3 categories not degraded, transition and degraded. There was minimal observation of human and livestock in the severely degraded classes. Similarly for Hallu, the livestock density was higher than the human density. Livestock distribution was predominant in the not degraded and degraded categories. Both the human and livestock population where minimal in the severely degraded category (Figure 10). Results from Seloto revealed a combination of high population densities for both human and livestock in the degraded and severely degraded classes with livestock numbers almost 6 times those of human on the overall (Fig. 10). The high livestock distribution within the severely degraded areas is a cause for concern in this area. There were similar observations noted for both Sabillo and Matufa. At all sites the human population densities were consistently lower than the livestock densities with the predominant degradation classes being degraded and severely degraded.

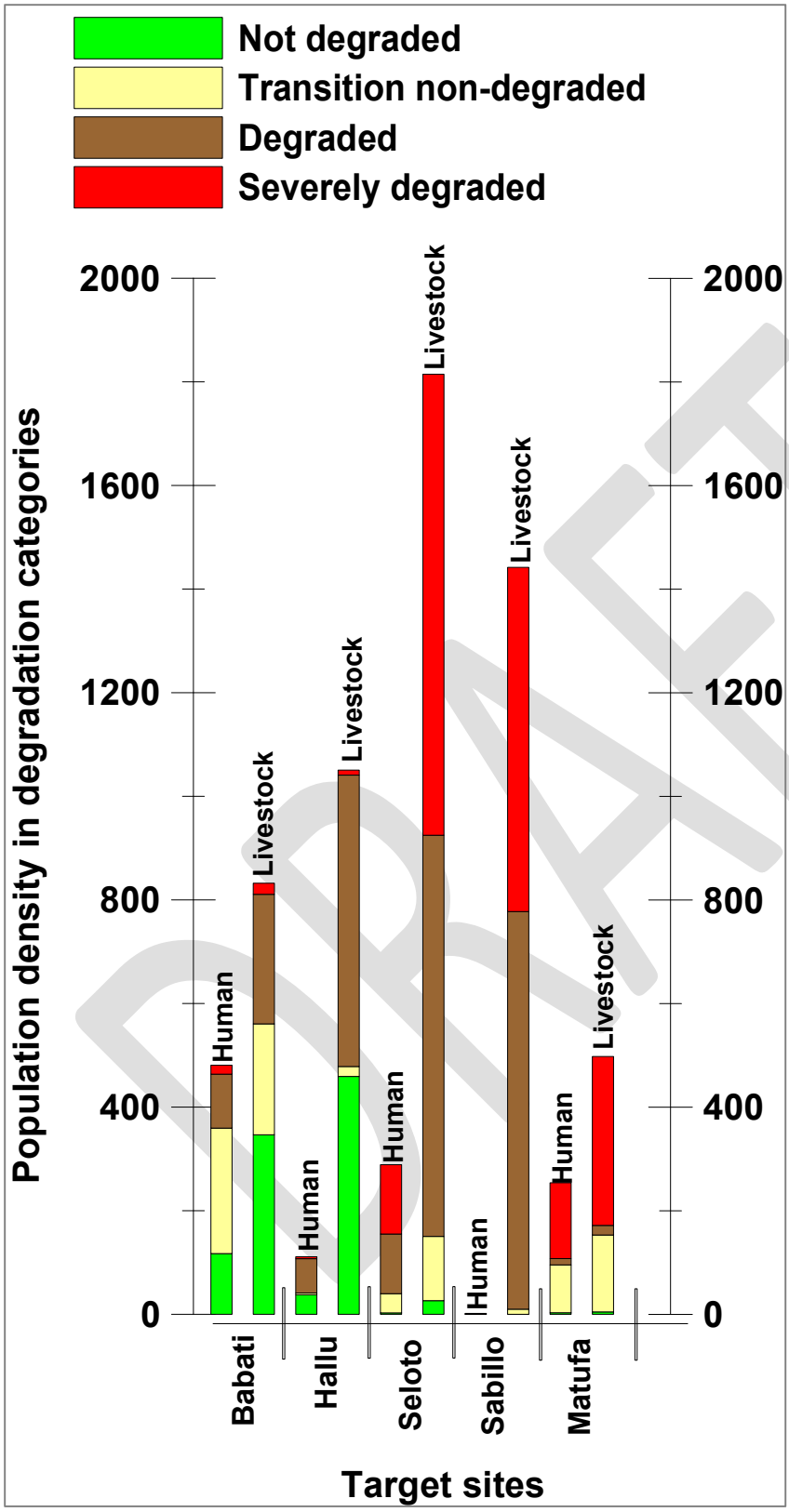

Figure.10: Representation of land degradation categories at target sites based on population density

This study demonstrated the construction of a geoprocessing model that accounts for both biophysical and socio-economic parameters to determine the erosion hazard over an area with subsequent assessment of land degradation status. The model produced intuitive and robust results that were validated with field visits which confirmed satisfactory prediction accuracy of up to 83%. Map study results revealed that a myriad of factors drive both erosion and land degradation part of which is a seasonal component (Figures 2, 3 and 7), the other being anthropogenic (Figures 7, 9 and 10). From the results of the seasonal variability analysis, it is clear that there is some transition between the erosion hazard classes as the seasons change. The direction of the transition indicated that it was the wet season that experiences higher class fragmentation compared to the dry season. However, the magnitude of these transitions is low and therefore we do not expect to see drastic differences in the erosion hazard classes' fragmentation between the dry and wet seasons.

For the case of the EHI, the maps (Figures 2 and 3) clearly showed that vulnerable features such as channels stand the greatest risk of erosion during the rainy season. The erosion hazard map for the dry season indicated population density (both human and livestock) as being a key determinant of EHI and was further evidenced by the high correlation matrix (Table 5). The correlation matrix revealed that the wet season erosion hazard is also strongly associated with biomass and land cover (Table 5). Examination of the correlation matrices allowed the identification of other major factors influencing erosion hazard in each season. These results suggest the need for a 2 pronged strategy to mitigate erosion risk from occurring. The dry season strategy would need to focus more around populated places such as areas surrounding large villages as well as areas with large herds of livestock especially because the observations revealed that land degradation appear to be predominantly population driven (both humans and livestock). On the other hand, the wet season strategy would need to focus more around vulnerable features such as road and river embankments as well as land use and land cover.

Based on trends observed in Fig. 9; the livestock footprint is quite big hence presenting missed opportunities for use of organic manures that help reduce soil chemical degradation. In addition, the use of forage buffer strips can help in reduction of erosion for environmental stability and restoration of soil functions. Considering that livestock was the predominant player in the dry season, options for use of irrigation towards forage production may reduce the dry season EHI. This has the potential to increase soil residue cover that also reduces rain drop impact during the wet season, allowing more time for water to infiltrate.

Study results indicate that significant portions of Babati District are agrarian yet about 50% of the region falls within both the degraded and severely degraded categories hence susceptible to erosion and degradation. Both the EHI and degradation levels presented in this study suggest that restoration options should consider both soil protection measures and soil fertility management strategies that should be implemented depending on the land use type, season and population density of a given area. Landscape diligence should be accorded to areas classified as transition zone non-degraded as these could be on the verge of potential degradation with very low fertility status, hence restoration options should emphasize soil fertility management but should not abandon or ignore soil protection.

The tools provided here for transformation of multi-criteria datasets on erosion risk and hazard into land degradation assessments provides the basis for undertaking and replicating this predictive modelling procedure to other areas, where largescale land degradation is of concern. The methods and results described in this study would be valuable for understanding the relationship between largescale soil erosion risk and land use planning towards avoided land degradation. For SSA, these are very important due to the current wave of activities involving land use conversion to other land cover types specifically forests and cultivated lands.

In conclusion, this multi-criteria approach resulted in the generation of spatial and quantitative information on erosion risk mapping and the creation of a land degradation assessment map from the combination of multiple parameters (soil chemical and physical degradation factors) interacting with each other that aided in the generation of the final quantitative degradation classes. The data showed that about 50% of the study area is prone to land degradation suggesting that the outputs of this modeling procedure can be used for the identification of land degradation levels that can in turn be used for targeted restoration benefits for areas of economic and environmental importance within landscapes. The tool can be added into the ArcGIS toolbox and can be accessed at: www.ciat.soils.net

References

Agele, D. T., Lihan, Sahibin, A. R., & Rahman, Z. A. (2013). Application of the RUSLE model inforecasting soil Erosion at downstream of the Pahang river basin, Malaysia. Journal of Applied Sciences Research, 9(1), 413-424.

Alexakis, D. D., Hadjimitsis, D. G., Agapiou, A., Themistokleous, K., & Papoutsa, C. (2012). Assessing soil erosion rate in a catchment area in Cyprus using remote sensing and GIS. Advances in Geosciences, 187-194. http://dx.doi.org/10.5194/hess-16-1321-2012

Arnold, J.G., Sirinivasan, R., Muttiah, R.S., Williams, J.R., (1998). Large area hydrologic modelling and assessment. Part 1: Model development. Journal of the American Water Resources Association, 34, 73-89.

Bakker, M. M., Govers, G., van Doorn, A., Quetier, F., Chouvardas, D., & Rounsevell, M. (2008). The response of soil erosion and sediment export to land-use change in four areas of Europe: the importance of landscape pattern. *Geomorphology*, *98*(3), 213-226.

Banai, R. (1993). Fuzziness in Geographical Information Systems: contributions from the analytic hierarchy process†. *International Journal of Geographical Information Science*, *7*(4), 315-329.

Berger, M., Belem, P. C., Dakoua, D., & Hien, V. (1987). Le maintien de la fertilite des sols dans l'quest du Burkina Faso et la necessite de l'association agriculturee levage. Cotton et Fibres Tropicales Vol XLII FASC, 3, 210-211.

Bishop-Sambrook C., Kienzle J., Mariki W., Owenya M. and Ribeiro F., 2004. Conservation Agriculture as a Labour Saving Practice for Vulnerable Households. Suitability of Reduced Tillage and Cover Crops for Households under Labour Stress in Babati and Karatu Districts, Northern Tanzania. IFAD and FAO

Boardman, J., Poesen, J., & Evans, R. (2003). Socio-economic factors in soil erosion and conservation. *Environmental Science & Policy*, *6*(1), 1-6.

Bork, H. R., & Lang, A. (2003). Quantification of past soil erosion and land use/land cover changes in Germany. In *Long term hillslope and fluvial system modelling* (pp. 231-239). Springer Berlin Heidelberg.

Brown, L. R. (1981). World population growth soil erosion and food security. *Science*, *214*(4524), 995-1002.

Bushan, N., Rai, K., 2004. Strategic Decision Making. Applying the Analytic Hierarchy Process

Carver, S. J. (1991). Integrating multi-criteria evaluation with geographical information systems. International Journal of Geographical Information System, 5(3), 321-339.

Cerdà, A. (2007). Soil water erosion on road embankments in eastern Spain.*Science of the Total Environment*, *378*(1), 151-155.

Cohen, J. (1960). A coefficient of agreement for nominal scales. Educational and Psychosocial Measurement, 20, 37-46.

Csáfordi, P., Pődör, A., Bug, J., & Gribovski, Z. (2012). Soil Erosion Analysis in a Small Forested Catchment Supported by ArcGIS Model Builder. Acta Silv. Lign. Hung., 8, 39-55. http://dx.doi.org/10.2478/v10303-012-0004-5

De Vente J., Poesen J., Bazzoffi P., Van Rompaey A. & Verstraeten G. (2006) Predicting catchment sediment yield in Mediterranean environments: the importance of sediment sources and connectivity in Italian drainage basins. Earth Surf. Proc. Land. 31, 1017–34.

de Vente, J., Poesen, J., Verstraeten, G., Van Rompaey, A., & Govers, G. (2008). Spatially distributed modelling of soil erosion and sediment yield at regional scales in Spain. *Global and planetary change*, *60*(3), 393-415.

Doran, J.W., Parkin, T.B., 1994. Defining and assessing soil quality. In Defining Soil Quality for Sustainable Environment., Doran JW et al 9eds). Special Publication No. 35. Soil Science Society of America: Madison, WI: 3-21.

Dyer JS (1990) Remarks on the analytic hierarchy process. Management Science 36(3).

Forman EH, Gass SI (2001). The analytic hierarchy process – an exposition. Operations Research

Forman, R. T., & Alexander, L. E. (1998). Roads and their major ecological effects. *Annual review of ecology and systematics*, 207-C2.

García-Ruiz, J. M. (2010). The effects of land uses on soil erosion in Spain: a review. *Catena*, *81*(1), 1-11.

Grepperud, S. (1996). Population pressure and land degradation: The case of Ethiopia. *Journal of environmental economics and management*, *30*(1), 18-33.

Hadley R. F., Lal R., Onstand C. A., Walling D. E. & Yair A. (1985) Recent Developments in Erosion and Sediment Yield Studies. Technical Documents in Hydrology by the working group of ICCE on the IHP-II Project. UNESCO, Paris, 1985.

Harden, C. P. (1992). Incorporating roads and footpaths in watershed-scale hydrologic and soil erosion models. *Physical Geography*, *13*(4), 368-385.

Hooke, J. M. (1979). An analysis of the processes of river bank erosion. *Journal of Hydrology*, *42*(1-2), 39-62.

Jiang, B., 2013. GIS-based time series study of soil erosion risk using the Revised Universal Soil Loss Equation (RUSLE) model in a micro-catchment on Mount Elgon, Uganda. Master degree thesis, Geomatics; Department of Physical Geography and Ecosystems Science, Lund University.

Jonsson, L.O., 1996. Rainwater management to avoid drought, IRD Currents no. 12, August 1996, pp 56-64

Komac, M. (2006). A landslide susceptibility model using the analytical hierarchy process method and multivariate statistics in perialpine Slovenia. *Geomorphology*, *74*(1), 17-28.

Kovář, P., Vaššová, D., & Hrabalíková, M. (2011). Mitigation of surface runoff and erosion impacts on catchment by Stone Hedgerows. Soil & Water Res., 6(4), 5-16.

Krull, E. S., Skjemstad, J. O., & Baldock, J. A. (2004). Functions of Soil Organic Matter and the effect on soil properties. GRDC report, Project CSO 00029. http://www.grdc.com.au/growers/res_summ/cso00029/contents.htm

Kumar, S., & Kushwaha, S. P. S. (2013). Modelling soil erosion risk based on RUSLE-3D using GIS in a Shivalik sub-watershed. Journal of Earth System Science, 122(2), 389-398. http://dx.doi.org/10.1007/s12040-013-0276-0

Lal, R., 2001. Soil degradation by erosion. Land Degradation and Development. 12: 519-539. DOI:10.1002/ldr.472

Lawrence P., Cascio A. L., Goldsmith P. & Abbott C. L. (2004) Sedimentation in Small Dams. Development of a Catchment Characterization and Sediment Yield Prediction Procedure. DFID Report. OD TN 120.

Lulseged Tamene, L., Abegaz, A., Aynekulu, A., Woldearegay, K., and Paul L. G. Vlek, PLG. (2011). Estimating sediment yield risk of reservoirs in northern Ethiopia using expert knowledge and semi-quantitative approaches. Lakes and Reservioirs Research and Management 16: 293-305.

Mallick, J., Alashker, Y., Mohammad, S. A., Ahmed, M., & Hasan, M. A. (2014). Risk assessment of soil erosion in semi-arid mountainous watershed in Saudi Arabia by RUSLE model coupled with remote sensing and GIS. Geocarto International. http://dx.doi.org/10.1080/10106049.2013.868044

Mendas, A. and Delali, A., 2012. Support system based on GIS and weighted sum method for drawing up of land suitability map for agriculture. Application to durum wheat cultivation in the area of Mleta (Algeria). Spanish Journal of Agricultural Research 2012 10(1): 34-43 ISSN: 1695-971-X eISSN: 2171-9292. Available online at www.inia.es/sjar doi: http://dx.doi.org/10.5424/sjar/2012101-293-11

Mohammadkhan, S., Ahmadi, H., & Jafari, M. (2011). Relationship between soil erosion, slope, parent material, and distance to road (Case study: Latian Watershed, Iran). *Arabian Journal of Geosciences*, *4*(1-2), 331-338.

Morgan, R.P.C, Quinton, J.N., Smith, R.E., GoversS, G., Poesen, J.W.A., Auerswald, K., ChisciI, G., Torri, D., Stychen, M.E., Folly, A.J.V. (1998). The European soil erosion model (EUROSEM): documentation and user guide. Silsoe College, Cranfield University.

Murage, E.W., Karanja, N.K., Smithson, P.C. and Woomer, P.L. (2000) Diagnostic indicators of soil quality in productive and non-productive smallholders' fields of Kenya's Central Highlands. Agriculture, Ecosystems and Environment 79, 1-8.

Musinguzi, P., Tenywa, J.S., Ebanyat, P., Tenywa, M.M., Mubiru, D.N., Basamba, T.A., Leip, A., 2013. Soil Organic Carbon Thresholds and Nitrogen Management in Tropical Agroecosystems: Concepts and Prospects. Journal of Sustainable Development; Vol. 6, No. 12; 2013. ISSN 1913-9063 E-ISSN 1913-9071. Published by Canadian Center of Science and Education. doi:10.5539/jsd.v6n12p31 http://dx.doi.org/10.5539/jsd.v6n12p31

Nearing MA, Foster GR, Lane LJ, Finkner SC. 1989. A process-based soil erosion model for USDA-Water Erosion Prediction Project technology. Transactions of the ASAE 32(5): 1587-1593.

Nekhay, O., Arriaza, M., & Boerboom, L. (2009). Evaluation of soil erosion risk using Analytic Network Process and GIS: A case study from Spanish mountain olive plantations. *Journal of environmental management*, *90*(10), 3091-3104.

Nunes, A. N., De Almeida, A. C., & Coelho, C. O. (2011). Impacts of land use and cover type on runoff and soil erosion in a marginal area of Portugal. *Applied Geography*, *31*(2), 687-699.

Othman, Z., & Ismail, W. R. (2012). Using environmental radionuclide, 137Cs to investigate soil re–distribution in an agricultural plot in Kalumpang, Selangor, Malaysia. Kajian Malaysia, 30(2), 45–70.

Parveen, R., & Kumar, U. (2012). Integrated approach of Universal Soil Loss Equation (USLE) and Geographical Information System (GIS) for soil loss risk assessment in Upper South Koel Basin, Jharkhand. Journal of Geographic Information System, 4, 588-596. http://dx.doi.org/10.4236/jgis.2012.46061

Pascual, U., & Barbier, E. B. (2006). Deprived land-use intensification in shifting cultivation: the population pressure hypothesis revisited. *Agricultural Economics*, *34*(2), 155-165.

Peter, K. D., d'Oleire-Oltmanns, S., Ries, J., Marzolff, I., & Hssaine, A. A. (2014). Soil erosion in gully catchments affected by land-levelling measures in the Souss Basin, Morocco, analysed by rainfall simulation and UAV remote sensing data. Catena, 113, 24-40. Retrieved from www.elsevier.com/locate/catena. http://dx.doi.org/10.1016/j.catena.2013.09.004

Prasannakumar, V., Vijith, H., Abinod, S., & Geetha, N. (2012). Estimation of soil erosion risk within a small mountainous sub-watershed in Kerala, India, using Revised Universal Soil Loss Equation (RUSLE) and geo-information technology. Geoscience Frontiers, 3(2), 209-215. Retrieved from www.elsevier.com/locate/gsf. http://dx.doi.org/10.1016/j.gsf.2011.11.003

PSIAC (Pacific Southwest Inter-Agency Committee) (1968) Factors affecting sediment yield and selection and evaluation of measures for the reduction of erosion and sediment yield. Pacific Southwest Inter-Agency Committee (PSIAC) report of the water management subcommittee, pp. 27.

Rabia, A.H., 2012. GIS Spatial Modeling for Land Degradation Assessment in Tigray, Ethiopia. 8th International Soil Science Congress on "Land Degradation and Challenges in Sustainable Soil Management", Çeşme -Izmir, Turkey. 2012. Ege University, May 15-17, volume 3, pp. 161:167.

Rambaldi, G APK Kyem, M Mccall and D Weiner. Participatory spatial information management and communication in developing countries. Electron. J. Inform. Syst. Develop. Countr. 2006; 25, 1-9.

Renard KG, Foster GR, Weesies GA, McCool DK, and Yoder DC (1997) Predicting soil erosion by water: a guide to conservation planning with the Revised Universal Soil Loss Equation (RUSLE). USDA Agricultural Handbook 703.

Ringo D.E., Mansoor H.A., Lyimo S.D., Minja M., Ngatoluwa R. and Olotu J., 2002. Refinement of Farming Systems and Agro-Ecological Zonations of Babati District and Development of Agricultural Resource Database, SARI, Arusha, Tanzania.

Sambrook, R. A., Pigozzi, B. W., & Thomas, R. N. (1999). Population pressure, deforestation, and land degradation: a case study from the Dominican Republic. *The Professional Geographer*, *51*(1), 25-40.

Schmoldt, D., Kangas, J., Mendoza, G. A., & Pesonen, M. (Eds.). (2013).*The analytic hierarchy process in natural resource and environmental decision making* (Vol. 3). Springer Science & Business Media.

Shakesby RA, Coelho COA, Schnabel S, Keizer JJ, Clarke MA, Contador JFL, Walsh RPD, Fereira AJD, Doerr SH. 2002. A ranking methodology for assessing relative erosion risk and its application to Dehesas and Montados in Spain and Portugal. Land Degradation & Development 13: 129–140.

Shi, X. Z., Wang, K., Warner, E. D., Yu, D. S., Wang, H. J., Yang, R. W., ... & Shi, D. M. (2008). Relationship between soil erosion and distance to roadways in undeveloped areas of China. *Catena*, *72*(2), 305-313.

Sparling, G. P., & Schipper, L. A. (2002). Soil quality at a national scale in New Zealand. Journal of Environmental Quality, 31, 1848-1857. http://dx.doi.org/10.2134/jeq2002.1848

Tamene L., Park S., Dikau R. & Vlek P. L. G. (2006a) Reservoir siltation in the semi-arid highlands of northern Ethiopia: sediment yield-catchment area relationship and a semi-quantitative approach for predicting sediment yield. Earth Surf. Proc. Land. 31, 1364– 83.

Tamene L., Park S., Dikau R. & Vlek P. L. G. (2006b) Analysis of factors determining sediment yield variability in the highlands of Northern Ethiopia. Geomorphology 76, 76–91.

Thiam AK. 2003. The causes and spatial patterns of land degradation risk in southern Mauritania using multitemporal AHVRR-NDVI imagery and field data. Land Degradation & Development 14: 133–142.

Todd, B. 2006. Assessment of Soil Erosion Risk within a Subwatershed using GIS and RUSLE with a Comparative Analysis of the use of STATSGO and SSURGO Soil Databases. Volume 8, Papers in Resource Analysis. 22pp. Saint Mary's University of Minnesota Central Services Press. Winona, MN. Retrieved 20 Oct 2015 from http://www.gis.smumn.edu

Trimble, S. W. (1997). Contribution of stream channel erosion to sediment yield from an urbanizing watershed. *Science*, *278*(5342), 1442-1444.

van Noordwijk, M., Cerri, C., Woomer, P.L., Nugroho, K. and Bernoux, M. (1997) Soil organic carbon dynamics in the humid tropical forest zone. Geoderma 79, 187– 225.

Van Oost, K., Govers, G., and Desmet, PJJ. (2000). Evaluating the effects of changes in landscape structure on soil erosion by water and tillage. Landscape Ecology 15 (6): 579591.

Van Rompaey, A., Bazzoffi, P., Jones, R.J.A. and Montanarella, L. (2005). Modelling sediment yields in Italian catchments. Geomorphology 65: 157-169.

Van Rompaey, A., Krasa, J. and Dostal, T. (2007). Modelling the impact of land cover changes in the Czech Republic on sediment delivery. Land Use Policy 24: 576-583.

Van Rompaey, A., Verstraeten, G., Van Oost, K., Govers, G. and Poesen, J. (2001). Modelling mean annual sediment yield using a distributed approach. Earth Surface Processes and Landforms 26 (11): 1221-1236.

Verstraeten, G. and Prosser, I.P. (2008). Modelling the impact of land-use change and farm dam construction on hillslope sediment delivery to rivers at the regional scale. Geomorphology 98: 199-212.

Verstraeten, G., Prosser, I.P. and Fogarty, P. (2007). Predicting the spatial patterns of hillslope sediment delivery to river channels in the Murrumbidgee catchment, Australia. Journal of Hydrology, 334: 440-454.

Verstraeten, G., Van Oost, K., Van Rompaey, A., Poesen, J. and Govers, G. (2002). Evaluating an integrated approach to catchment management to reduce soil loss and sediment pollution through modelling. Soil Use and Management, 18: 386-394.

Wischmeier WH and Smith DD (1978) Predicting rainfall erosion losses: A guide to conservation planning, Agriculture Handbook No. 537, U.S. Department of Agriculture, Washington D.C., 58 p.

Wolman, M. G. (1967). A cycle of sedimentation and erosion in urban river channels. *Geografiska Annaler. Series A. Physical Geography*, 385-395.

Wu, Q., & Wang, M. (2007). A framework for risk assessment on soil erosion by water using an integrated and systematic approach. Journal of Hydrology, 337(1), 11-21.

Yalcin, A. (2008). GIS-based landslide susceptibility mapping using analytical hierarchy process and bivariate statistics in Ardesen (Turkey): comparisons of results and confirmations. Catena, 72(1), 1-12.

Zuazo, V. H. D., & Pleguezuelo, C. R. R. (2008). Soil-erosion and runoff prevention by plant covers. A review. Agronomy for sustainable development, 28(1), 65-86.

Annex I: Factors considered in derivation of the Erosion Hazard Index

Model design: In this study, the following sub-models were constructed to model the fundamental factors influencing erosion hazard:

Topography – this sub-model evaluates the terrain of the study area to identify areas with steep gradients where it is much easier for the agents of erosion to carry away soil. It therefore requires slope data which is generated from a DEM. The sub-model also looks at the stream power index for the terrain, a parameter used to define potential flow erosion at a given point of the surface. The stream power index is determined by the upslope catchment area and the gradient of the slope, which together determine the volume and velocity of water flow over a surface and thus the erosion risk.

Soil characteristics – this sub-model evaluates the susceptibility of the soil to erosion. This is determined by the texture of the soil. Coarse texture soils like sand are more susceptible to erosion compared to fine texture soils like clay. This model evaluates the proportions of clay, silt and sand in the soil of an area to determine areas with higher erodibility.

Rainfall – this sub-model evaluates the rainfall patterns over the study area to determine erosivity over the study area. Precipitation plays a major role in the model due to the kinetic energy of rainfall. This sub-model allows the erosivity of different parts of the study area to be included as a factor in the model.

Land cover and use – this sub-model determines the exposure of the land to agents of erosion. The vegetation density over an area is estimated using biomass, which is obtained from an NDVI layer. Places with higher biomass are considered to be better protected from erosion than similar areas but with lower biomass. Also evaluated is the use that the land has been put to. Land under natural vegetation use such as forests tends to have less soil disturbance and so is less vulnerable to erosion. Conversely crop land tends to have more disturbed soil which increases its vulnerability to erosion.

Vulnerable features – this sub-model evaluates linear features that are vulnerable to erosion such as roads and seasonal rivers which typically have steep exposed earthen walls. Run-off typically follows the drainage channels established by such linear features resulting in progressive erosion of the walls bounding these features. Aside from the channels that characterize such features, they also attract human activity due to the services they offer. For instance, roads facilitate transport and thus attract human activity, while rivers do the same by providing water. The nearer an area is to such features, the more its ground is affected by anthropogenic activity making it increasingly vulnerable to erosion. This sub-model includes such features into the analysis to identify areas at higher erosion hazard due to the presence of such features.

Population density – this sub-model evaluates the erosion risk contributed by human and animal populations residing in an area. The higher the population of people, the more the activities that increase erosion hazard such as the building of features such as roads and conversion of land use from natural classes to cropland. Similarly, the higher the livestock density, the greater the demand for pasture which increases probability of overgrazing and thus erosion risk.

Addendum 1: Field Validation data points.

PointID	Latitude	Longitude	LandUse	Biomass	Slope	ErosionHazard
1.000000	-4.23201806582	35.84017238730	Natural	High	Low	Low
2.000000	-4.19157212380	36.02628137900	Natural	Low	Low	High
3.000000	-4.20068792932	35.75696175380	Anthrop	Low	Low	High
4.000000	-4.09911792841	35.90056000750	Natural	Low	Low	High
5.000000	-3.83675243365	35.95691123730	Natural	Medium	Low	Low
6.000000	-4.29496065820	35.40190630400	Anthrop	Low	Low	High
7.000000	-3.88784497786	35.94274175650	Natural	Medium	Low	Medium
8.000000	-3.87368560991	35.86132156950	Mixed	Low	Low	High
9.000000	-4.25611716318	35.80541861320	Natural	High	High	Low
10.000000	-4.09364915711	35.66573346020	Anthrop	Medium	Low	Medium
11.000000	-3.80370343027	35.92878172400	Natural	Medium	Low	Medium
12.000000	-3.71777313746	35.96979530200	Mixed	Low	Low	High
13.000000	-4.26085538892	35.62714954030	Anthrop	Medium	Medium	Medium
14.000000	-4.22747921333	35.27707003270	Anthrop	Low	Low	High
15.000000	-4.01770780155	35.70795816440	Natural	Low	Low	High
16.000000	-4.01990971214	35.84598612810	Natural	High	Medium	Low
17.000000	-4.18680863801	35.37184421690	Anthrop	Low	Low	High
18.000000	-4.14226375275	36.08992959280	Natural	Medium	Low	Medium
19.000000	-4.22857472148	35.69292561210	Natural	Low	High	High
20.000000	-4.17958200034	35.95530413240	Natural	Medium	Low	High
21.000000	-4.21836348396	35.93599453750	Anthrop	Low	Low	High
22.000000	-3.88224683377	35.71313470830	Mixed	Low	Low	High

23.000000	-4.05527261744	35.71164573820	Anthrop	Medium	Medium	Medium
24.000000	-4.22561308559	35.89179001930	Anthrop	Low	Low	Low
25.000000	-4.20838513801	35.55127352570	Anthrop	Medium	Medium	Medium
26.000000	-4.34315960419	35.78125996130	Natural	High	Medium	Low
27.000000	-4.02610074532	36.10700052540	Natural	Low	Low	High
28.000000	-4.16331170637	35.94695279880	Natural	Low	Low	High
29.000000	-4.18629102918	35.44495670070	Anthrop	Low	Low	Medium
30.000000	-4.22300528337	35.68538497590	Natural	High	High	High
31.000000	-4.12959791440	36.18005732430	Natural	Medium	Medium	Medium
32.000000	-4.35315782497	35.42992906310	Mixed	Medium	Medium	Medium
33.000000	-4.31601510571	35.72806879210	Anthrop	High	Low	Low
34.000000	-4.20386950590	35.91110906070	Anthrop	Medium	Low	Low
35.000000	-4.02151900861	35.74074122980	Anthrop	Low	Low	High
36.000000	-4.14087648512	35.65870228310	Anthrop	Medium	Medium	High
37.000000	-4.29337496335	35.26637136080	Mixed	Low	Low	High
38.000000	-4.21106087286	35.99172890760	Natural	Low	Low	High
39.000000	-4.16350933444	36.21534853210	Natural	Low	Low	Medium
40.000000	-3.91488487790	36.07404982950	Natural	Low	Low	High